Chemistry and Physics of Lipids 218 (2019) 125–135

Contents lists available at ScienceDirect

Chemistry and Physics of Lipids

journal homepage: www.elsevier.com/locate/chemphyslip

# Interactions of valproic acid with lipid membranes of 1,2-dimyristoyl-*sn*-glycero-3-phosphocholine

F. Corrales Chahar[a], S.B. Díaz[b], A. Ben Altabef[b,c,*], C.A. Gervasi[d,e,**], P.E. Alvarez[a,c,***]

[a] Instituto de Física, Facultad de Bioquímica, Química y Farmacia. UNT, Ayacucho 471, 4000 Tucumán, Argentina
[b] Instituto de Química Física, Facultad de Bioquímica, Química y Farmacia. UNT, San Lorenzo 456, T4000CAN S. M. de Tucumán, Argentina
[c] Instituto de Química del Noroeste Argentino (INQUINOA)-CONICET-Tucumán, Argentina
[d] INIFTA-CONICET, Facultad de Ciencias Exactas, UNLP, Suc. 4-C.C. 16. (1900) La Plata, Argentina
[e] Area Electroquímica, Facultad de Ingeniería, UNLP, 1 y 47 (1900) La Plata, Argentina

ARTICLE INFO

*Keywords:*
Valproic acid
Lipid membrane
FTIR
Raman
EIS

ABSTRACT

Lipid bilayers of 1,2-dimyristoyl-*sn*-glycero-3-phosphocholine (DMPC) were prepared in two forms, as a suspension of multilamellar spherical vesicles and as planar membranes deposited on a conductive solid support. We used Fourier Transformed Infrared (FTIR) and Raman spectroscopic techniques to study the lipid vesicles while the solid supported bilayers were characterized by using electrochemical experiments (cyclic voltammetry and impedance). Valproic acid (Valp) was either present in the solution or incorporated into the lipid structure. As the Valp:DMPC ratio increases the phase transition temperature decreases while the phase transition becomes less marked. Moreover, for the Valp:DMPC complex species a slight decrease in the number of *gauche* isomers was observed relative to the number of *trans* isomers what corresponds to an increase in the packing density of the acylic chains. Based on derived electrical properties of the supported membranes it can be concluded that Valp induces the formation of pores and other defects in the lipid films. Valp incorporated into the membrane is seriously detrimental to the bilayer stability.

## 1. Introduction

Drug-membrane interactions have attracted considerable attention since these interactions are known to affect the structure and properties of biological membranes strongly. A large number of distinguishing qualities of a membrane can be modified by means of an interaction with drugs (El Kirat et al., 2010; MacCallum and Tieleman, 2008). Some of the membrane traits that can be modified upon interaction with drugs are: the conformation of acyl groups, the membrane surface and thickness, the phase transition temperature, the membrane potential and hydration of the head groups and finally, the membrane fusion properties.

The bilayers of phospholipids can be considered as model systems of cell membranes since they preserve their two-dimensional fluidity and can be modified with membrane proteins, ion channels, receptors, transporters and can be used in many applications in the field of biotechnology (Martin, 2007; Chan and Boxer, 2007). Liposomes, in which the composition, structure and dynamics of phospholipids can be completely controlled, are generally recognized as models for in vitro studies of the properties and structure of cell membranes. Even a pure hydrated phospholipid bilayer is highly complex, and poses challenges for performing experiments and computation. Membranes of DMPC are among the most studied systems, as DMPC has been widely characterized both experimentally and computationally (Juhaniewicz and Sek, 2015). On the other hand, liposomes of 1,2-dipalmitoyl-sn-glycero-3-phosphocholine (DPPC) were used as drug delivery vehicles and their delivery efficacy was tested for 5-ALA-medicated PDT, both *in vitro* and *in vivo*. Moreover, DPPC liposomes can act as carriers for hydrophilic drugs such as 5-ALA. Due to its hydrophilic properties, 5-ALA can be entrapped in the aqueous phase of liposomes and this brings about the limitation of the entrapment efficiency (Lin et al., 2016). Additionally, lipid bilayers supported on gold surfaces are also interesting models for cell membranes. Electrochemical techniques are widely accepted as ideally suited tools to characterize membranes supported on a

* Corresponding author at: Instituto de Química Física, Facultad de Bioquímica, Química y Farmacia. UNT, San Lorenzo 456, T4000CAN S. M. de Tucumán, Argentina.
** Corresponding author at: INIFTA-CONICET, Facultad de Ciencias Exactas, UNLP, Suc. 4-C.C. 16. (1900) La Plata, Argentina.
*** Corresponding author at: Instituto de Física, Facultad de Bioquímica, Química y Farmacia. UNT, Ayacucho 471., 4000 Tucumán, Argentina.
*E-mail addresses:* altabef@fbqf.unt.edu.ar (A. Ben Altabef), gervasi@inifta.unlp.edu.ar (C.A. Gervasi), palvarez@fbqf.unt.edu.ar (P.E. Alvarez).

https://doi.org/10.1016/j.chemphyslip.2018.12.010
Received 11 October 2018; Received in revised form 6 December 2018; Accepted 20 December 2018
Available online 21 December 2018
0009-3084/ 

conductive solid (Diamanti et al., 2016; Diamanti et al., 2017). In particular, impedance experiments provide a measurement of the dielectric properties of the system and their changes related to the interaction with different biomolecules (Steinem et al., 2000; Du et al., 2006; Rameshkumar and Kumaravel, 2017; Corrales Chahar et al., 2018). Many excellent reviews are readily accessible from the literature (Vallejo and Gervasi, 2006; Ziebert and Lacoste, 2011) where the subject is thoroughly discussed.

Valproic acid (Valp), on the other hand, is a branched short-chain fatty acid with broad-spectrum anticonvulsant activity that has been used since the 1970s for the treatment of generalized epilepsy and for the treatment of other diseases, such as bipolar disorders and migraines. After more than 40 years of clinical use, the mechanisms of action of Valp are still not fully understood (Rosenberg, 2007). Due to its anticonvulsant activity against a broad spectrum of different types of seizures, it has been frequently suggested that Valp acts through a combination of several mechanisms. Different studies suggest that Valp anticonvulsant action results from its effect on the neurotransmission mediated by gamma-aminobutyric acid (GABA) in the brain (Johannessen and Johannessen, 2003). Other studies suggest that Valp anticonvulsant action is the result of its effect on sodium and potassium channels, but these data were described as inconsistent (Loscher, 1999). Valp does not have a known specific binding site on the plasmatic membrane, which suggests that can act directly on the membrane, possibly as a disruptive agent. This suggestion is supported by several studies (Keane et al., 1983). These studies have shown that the anticonvulsant potency of Valp analogues increases according to their chain length and water / octanol partition coefficient. The latter fact suggests that the activity of Valp analogues depends on their lipophilicity. It has been discovered that Valp and analogous compounds (Lyon and Goldstein, 1980) are agents that alter the membrane and that the ability to perturb the membrane *in vitro* correlates with their anticonvulsant activity (Kessel et al., 2001).

The static and kinetic properties of valproic acid that interact with lipid bilayers of fully hydrated dipalmitoyl phosphatidylcholine were studied using molecular dynamics simulations (Ulander and Haymet, 2003). These authors present spatially resolved free energy calculations for the transport of valproic acid and valproate molecules across hydrated DPPC lipid bilayers. They observed the formation of a large water defect when valproate is located in the center of the membrane.

In this work we intend to gain a deeper insight into the effects of the interaction between valproic acid and lipid bilayer membranes of 1,2-Dimyristoyl-*sn*-glycero-3-phosphocholine (DMPC) (Fig. 1). To achieve this goal we used Fourier Transformed Infrared (FTIR) and Raman spectroscopic techniques and electrochemical experiments (cyclic voltammetry and impedance).

## 2. Experimental

### 2.1. Lipids and chemicals

1,2-dimyristoyl-*sn*-glycero-3-phosphocholine (DMPC) from Avanti-Polar Lipids, positively-charged dimethyldioctadecylammonium chloride (DODAC) and Tris (tris-hydroxymethyl aminomethane) with a purity ≥ 99.8% were purchased from Sigma–Aldrich Inc. (St. Louis, MO, USA); 3-mercaptopropionic acid (MPA) from Merck (Germany), valproic acid (Valp) from Sigma-Aldrich (Argentina). All other chemicals were of analytical grade, and tridistilled water was employed in all the experiments.

### 2.2. Lipid sample preparation

Multilamellar vesicles (MLVs) were prepared of DMPC and DMPC:Valp at different molar ratios, following Bangham's method (Bangham et al., 1974). The pure lipid and the Valp:DMPC samples at different molar ratios (0.42:1, 0.84:1 and 1.69:1) were dissolved in chloroform and dried under a stream of nitrogen to form a lipid film. The samples were kept for 24 h under vacuum, to ensure complete elimination of the solvent. The samples of the Valp:DMPC complexes were rehydrated and suspended in tridistilled water. On the other hand, a fraction of the pure lipid samples was rehydrated in aqueous solution of Valp in 7 mM concentration. The aqueous solution was prepared with tridistilled water and the concentration of 7 mM was chosen since it is the maximum concentration at which Valp is soluble in water.

The mechanical dispersion of the hydrated lipid films was obtained under vigorous shaking for 15 min, resulting in an opalescent suspension of MLVs, at room temperature. The final lipid concentration was 50 mg/mL.

### 2.3. Preparation of supported lipid bilayers (SLBs) on Au

Unlike a vesicle or a cell membrane in which the lipid bilayer is rolled into an enclosed shell, a supported bilayer is a planar structure sitting on a solid support. Because of this, only the upper face of the bilayer is exposed to the free solution. One of the great advantages of the supported bilayer geometry is its enhanced mechanical stability. SLBs will remain largely intact even when subjected to either high flow rates of an adjacent fluid or vibration. Moreover, the presence of holes will not destroy the entire bilayer (Purrucker et al., 2001). SLBs were obtained by attaching the lipid bilayer, containing a fraction of a positively-charged lipid, to the surface of a gold electrode modified with a negatively-charged self-assembled monolayer of MPA (Plant,1993). For this purpose, the electrode was incubated for at least 1 h in an ethanolic solution of 0.1 M MPA.

The final lipid film (Bangham et al., 1974) was prepared from mixtures of: 80% DMPC and 20% DODAC, which is positively charged.

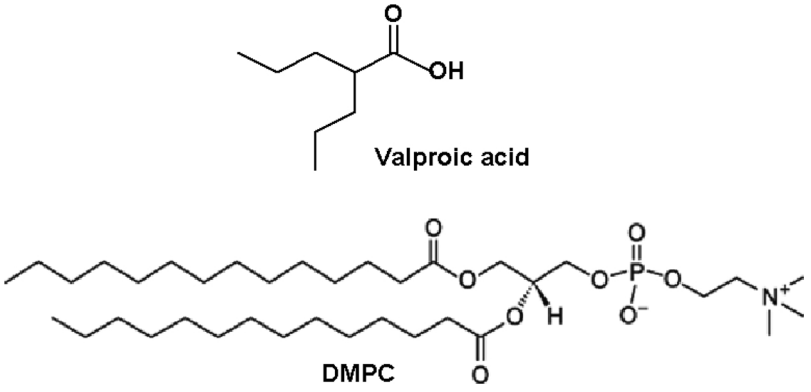


**Fig. 1.** Chemical structures of 1,2-Dimiristoyl-sn-glycero-3-phosphatidylcholine (DMPC) and Valproic Acid (Valp) molecules used in this study.

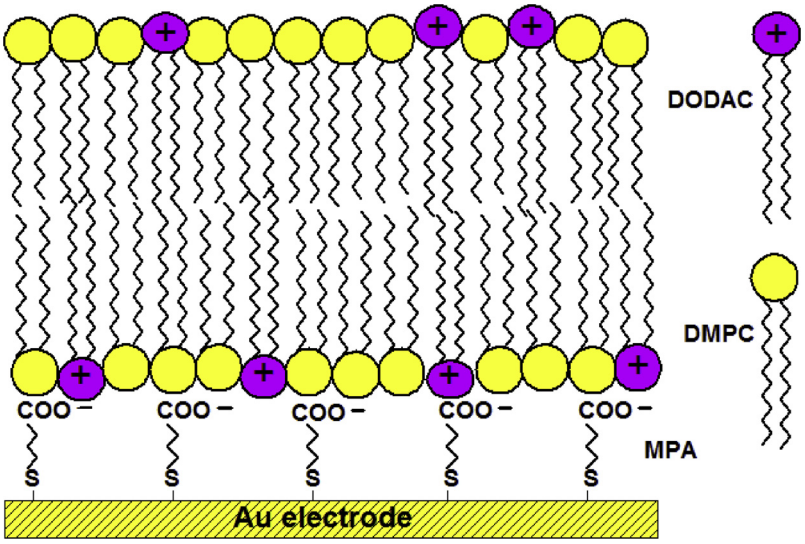


**Fig. 2.** Diagram of a supported bilayer [Alvarez et al., 2007].

In this way, the lipid bilayer was successfully deposited on the modified solid substrate thanks to electrostatic forces of attraction.

To obtain bilayer structures with incorporated Valp, lipid films of the Valp:DMPC complexes were used to prepare mixtures containing 20% DODAC. MLVs were formed by vigorous shaking and rehydration of the film in the presence of 10 mM Tris buffer solution with 0.1 M potassium chloride (KCl), pH 7.4. A suspension of multilamellar vesicles with a final concentration of 3% w/v was obtained. To ensure that only a single lipid bilayer became attached to the gold surface, the MLV suspension was extruded by using a LIPEX™ Extruder, (Bergera et al., 2001; Olson et al., 1979). In this way, a suspension of unilamellar vesicles (LUVs) was obtained, with which the electrode, containing the MPA self-assembled monolayer, was incubated for at least 15 h (Fig. 2). Thus, lipid bilayers were deposited by vesicle fusion on Au substrates through electrostatic binding with the previously assembled monolayer of MPA.

### 2.4. FTIR and Raman spectroscopic measurements

#### 2.4.1. FTIR measurements

FTIR measurements were carried out in a Perkin Elmer GX spectrophotometer, with a DTGS detector. The spectra of biomolecules with the phospholipid were acquired in a demountable cell for liquid samples with ZnSe windows. The temperature of the cell was controlled within the 12 °C–35 °C range by using a Peltier-type system with an accuracy of ± 0.1 °C. The resolution of the spectrophotometer was 1 $cm^{-1}$. A total of 64 scans were recorded in each condition and the spectra were analyzed using the OMNIC v.7.2 mathematical software provided by the manufacturer.

Using FTIR, the phase transition temperature ($T_m$) of the DMPC from gel phase to liquid-crystalline phase and the influence of Valp on $T_m$ were determined (Casal and Mantsch, 1984).

The bands in the mixtures were assigned to the carbonyl and phosphate groups by comparison with pure lipids. The C═O bands, are broad and overlapping. The Fourier deconvolution was used to estimate the frequencies of the component bands, followed by curve-fitting to obtain the bandwidth and the intensity (band narrowing factors: 1.6–2.2).

Deconvolution was used to obtain the peak frequencies of the component bands reported for the two populations of carbonyls in the lipid: the non-hydrated (1737 $cm^{-1}$) and the hydrated (1722 $cm^{-1}$) populations in the fluid state (Disalvo et al., 2002; Arias et al., 2015; Arias et al., 2018). The changes of these two populations were studied according to the molar ratio Valp:DMPC, both in the gel state and in the liquid crystalline state.

#### 2.4.2. RAMAN measurements

Vibrational Raman spectra of the samples were recorded by using a confocal Thermo Scientific-DXR Raman Microscope. The microscope is equipped with a high resolution motorized platen, a set of Olympus optical objectives, lighting module bright field/dark field trinocular viewer and an Olympus camera of 2048 pixels with CCD detector. The confocal system is real, with opening/hole matched with the point of symmetry of the excitation laser. The resolution is 2 µm in depth profiles. The standard spatial resolution was better than 1 µm.

The spectra were obtained at room temperature, by using a laser diode-pumped solid state (DPSS) of 532 nm with a power of 10 mW; the optical objective used was a 10X with an optical opening of 25 µm. The spectra were analyzed by using the OMNIC™ program for Dispersive Raman.

### 2.5. Electrochemical measurements

A three-electrode cell was used for the electrochemical experiments that were performed with a Zahner IM6 electrochemical workstation. The area of the Au working electrode was 1 $cm^2$. A platinum sheet served as the counter electrode while the reference electrode was a saturated calomel electrode (SCE). All potentials in this work are referred to the SCE (0.2412 V with respect to the normal hydrogen electrode). Cyclic voltammetry was recorded at a sweep rate v = 50 mV $s^{-1}$. The frequency range for recording impedance spectra covered from 30 kHz to 0.01 Hz with a perturbation signal amplitude of 10 mV. Experimental spectra were measured at the open circuit potential.

## 3. Results/Discussion

### 3.1. Vibrational spectroscopy measurements

The interactions between the lipid membranes of DMPC and Valp were studied by using Fourier Transform Infrared (FTIR) spectroscopy. The obtained spectra were comparatively analyzed by a study of the spectral bands corresponding to the inner and interphase regions of the lipid bilayer.

The FTIR spectra of MLVs of pure DMPC and Valp:DMPC complexes at different molar ratios are shown in Figs. 3 and 4. The spectra were recorded at 18 °C (gel state) and at 31 °C (liquid-crystalline state). The pure Valp spectrum is also shown. In all the graphs, the signals of the bands corresponding to the different functional groups of interest were

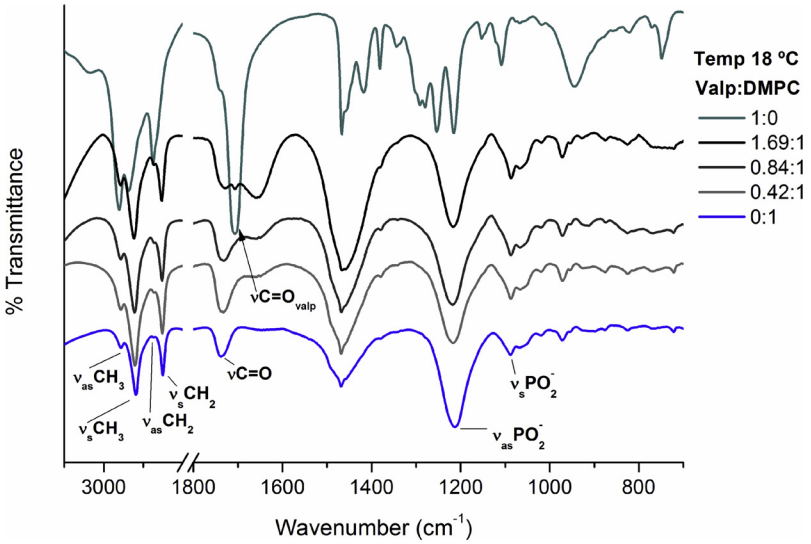


**Fig. 3.** Assignment of the bands in FTIR spectra of MLVs of pure DMPC (blue), Valp:DMPC complexes in different molar ratios (gray gradient) in the gel state and pure Valp (green).

assigned.

The spectra corresponding to the MLVs of DMPC, obtained by re-suspending the lipid film in a 7 mM Valp solution and resulting in a molar ratio of Valp:DMPC of 0.094:1 are presented in Figures S1 and S2.

*3.1.1. Influence of Valp on the phase transition temperature of the DMPC*

DMPC is a saturated lipid, with fatty acid chains of 14 carbon atoms (14:0/14:0), whose phase transition temperature ($T_m$), from gel to crystalline liquid state, is 23 °C (Heimburg, 2007; Garcia-Manyes et al., 2005). The changes in the wavenumber of the symmetric stretch of the methylene group ($\nu_s$ $CH_2$) were recorded in the FTIR spectra of MLVs of pure DMPC in a temperature range between 12 °C and 35 °C A $T_m$ value of 23 °C for DMPC is determined with the first derivative of the curve obtained by plotting the wave number of the symmetric stretch of $CH_2$ as a function of the sample temperature (**Figure S3**).

The asymmetric stretching vibrations around 2922 $cm^{-1}$ ($\nu_{as}$ $CH_2$) can also be used for this determination since they produce practically the same results. The main phase transition is also observed through changes in other parameters of the band, such as bandwidth and peak height [Cameron et al., 1980].

In Figs. 5(a) and (b), the wavenumber corresponding to $\nu_s$ $CH_2$ is represented as a function of the sample temperature for different conditions of the two studied Valp-DMPC systems. In Fig. 5(a), no change is observed in the $T_m$ of the lipid when the MLVs of DMPC are re-suspended in the 7 mM valproic acid solution for different exposure times (1 h, 24 h and 192 h) after the vesicles formation. Fig. 5(b) shows results corresponding to samples of the Valp:DMPC complex, in which Valp was incorporated directly into the lipid film, in different molar ratios, before forming the liposomes. A significant effect is observed related to the action of the drug characterized by a decrease in the $T_m$ of the lipid, as the molar ratio Valp:DMPC increases while the phase transition becomes less noticeable.

The effect produced by different substances on the $T_m$ of a lipid has been studied by different techniques for a long time, (Cameron et al., 1980; Cortijo and Chapman, 1981; Mannock et al., 2006) being the influence of cholesterol on the $T_m$ a model case. The presence of cholesterol in lipid membranes of DMPC causes shifts in band frequencies

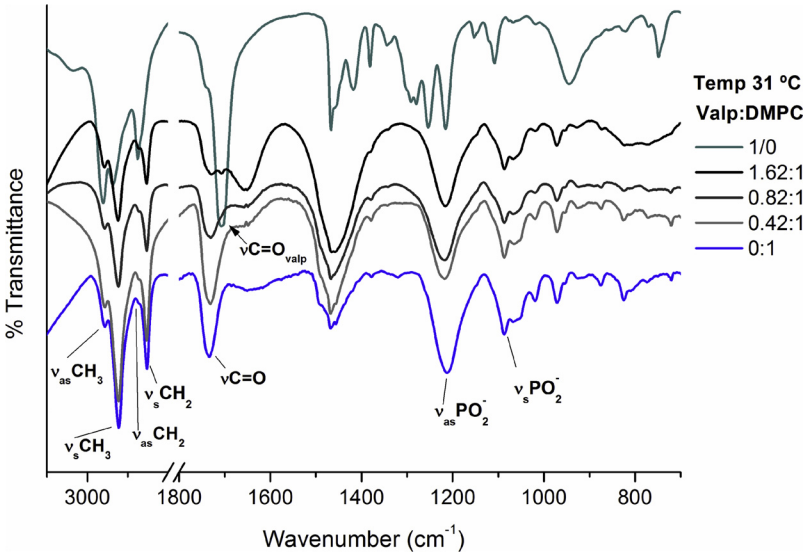


**Fig. 4.** Assignment of the bands in FTIR spectra of MLVs of pure DMPC (blue), Valp:DMPC complexes in different molar ratios (gray gradient) in liquid-crystalline state and pure Valp (green).

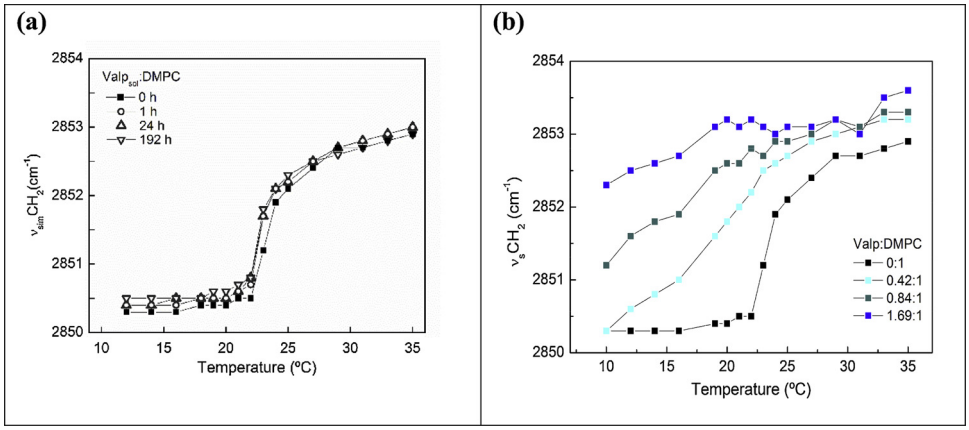


**Fig. 5.** Graphs of the wavenumber of the band corresponding to $\nu_s$ $CH_2$ as a function of the sample temperature in MLV spectra: (a) Valp in solution for different exposure times and (b) Valp incorporated into the vesicles at different molar ratios.

which indicate that an increase in the number of *gauche* conformers occurs below $T_m$ (less order) and a decrease in this number occurs above $T_m$ (more order) [Cortijo and Chapman, 1981]. Here (Fig. 5(b)), the incorporation of Valp in the lipid bilayer results in a more complex effect than that reported for cholesterol. The presence of Valp causes an increase in the average number of *gauche* isomers below the temperature $T_m$, which increases for higher Valp:DMPC molar ratios, thus the hydrocarbon chains would have greater freedom of movement. Above the $T_m$ there is a slight increase in the number of *gauche* isomers with respect to the pure lipid at these temperatures. It is observed that, at temperatures above the transition temperature $T_m$, the effects of disorder due to the presence of Valp are added to that of the higher temperatures examined.

Figs. 6(a) and (b) show the FTIR bands that illustrate the changes, induced by temperature and by the presence of Valp, in the DMPC spectra in the region of 3000 to 2800 cm$^{-1}$. At temperatures below the $T_m$ (18 °C), an increase in bandwidth and a wavenumber shift (≈3 to 4 cm$^{-1}$) of these bands are observed, which reflects an increase in mobility and in the content of rotamers in the hydrocarbon chains (Bilge et al., 2013; Ergun et al., 2014). At temperatures above the $T_m$ (31 °C), a slight increase in the width of the bands is observed, without a considerable change in the wavenumbers.

### 3.1.2. Hydrophobic region

*3.1.2.1. FTIR measurements.* Tables S1 and S2 show the assignments of the bands and the changes in the wavenumbers of the vibrations of the symmetric and asymmetric stretches of the methyl and methylene groups, of the hydrocarbon chains inside the lipid bilayer, at 18 °C (gel state) and at 31 °C (crystalline liquid state).

Table S1 shows the effect of Valp incorporated into the lipid bilayer. It is observed that the interaction between Valp and the hydrocarbon chains of DMPC is more evident in the gel state than in the crystalline liquid state, where it is practically null. In the gel state, changes in the wavenumbers of the bands of $\nu_s CH_2$ and $\nu_{as} CH_2$ are more significant as the molar ratio between Valp:DMPC increases. In Table S2, no interaction is observed for the MLVs resuspended in Valp solution, in both states.

### 3.1.3. Hydrophilic region

*3.1.3.1. FTIR measurements.* The interfacial region is strongly dependent on the hydration status of the lipid bilayer and susceptible to hydrogen bonds (Disalvo et al., 2008). The analysis of the FTIR spectra obtained for the MLVs of the Valp:DMPC complexes allowed to characterize the hydrophilic region by considering the wavenumber changes of the vibration bands of the stretches C═O and $PO_2^-$ in comparison with the corresponding bands of pure DMPC.

*3.1.3.2. C═O group.* It has been reported that the main ν C═O peak in diacyl lipids can be split in two components that correspond to the ν C═O vibrational modes of non-bonded (free) and H-bonded (bond) conformers of the C═O group (Hübner and Blume, 1998; Dıaz et al., 2003).

To investigate the H-bond interactions between Valp and the C═O groups in lipid vesicles of DMPC, a deconvolution of the main band of νC═O (both for the gel state and for the crystalline liquid state) was carried out which resulted in three components: $\nu C = O_{bond}$, $\nu C = O_{free}$ and $\nu C = O_{valp}$. The higher wavenumber band component (1744 cm$^{-1}$ at 18 °C and 1744 at 31 °C) was assigned to the free νC = O groups (ν C = $O_{free}$), whereas the lower wavenumber component (1734 cm$^{-1}$ at 18 °C and 1734 at 31 °C) was attributed to the νC = O vibration of H-bonded conformers ($\nu C = O_{bond}$) in DMPC liposomes.

The graphs of the deconvolutions of the bands of the C═O groups in

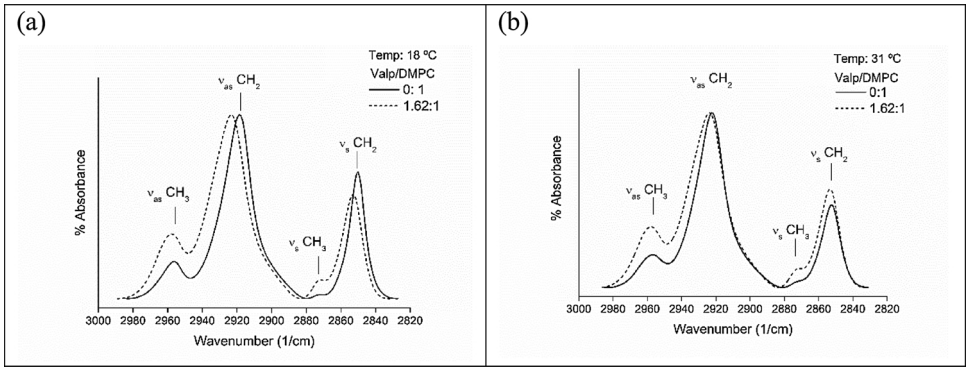


**Fig. 6.** FTIR spectra of MLVs of pure DMPC and complexes Valp:DMPC, (a) at 18 °C and (b) at 31 °C, in the C–H stretching region.

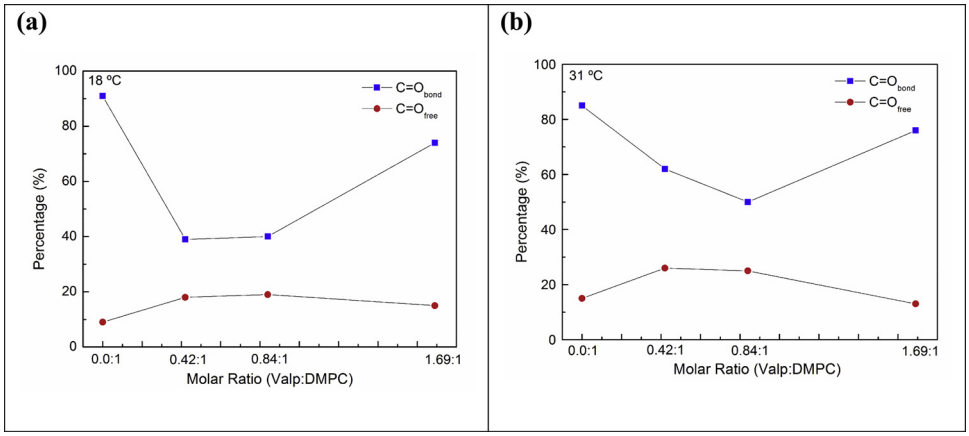


**Fig. 7.** Contribution of $\nu C = O_{free}$ and $\nu C = O_{bond}$ to the carbonyl population in different molar ratios of Valp:DMPC and at 18 °C (a) and 31 °C (b).

the MLVs vesicles of DMPC resuspended in a solution of Valp 7 mM and with Valp incorporated in the lipid bilayer, at different molar ratios, in the gel and crystalline liquid state, are presented in Figures S4 and S5, respectively. The assignments of the component bands are reported in Tables S3 and S4.

It is observed that the variations in the values of the wavenumbers assigned to bands are small for all Valp:DMPC molar ratios, both in the gel and in the liquid crystalline state (Table S4). For both analyzed temperatures, the increase in intensity of the band assigned to the population of the carbonyls linked to hydrogen bridges is remarkable (C═O bond).

Fig. 7 shows the percentage contribution of $C{=}O_{bond}$ and $C{=}O_{free}$ to the carbonyl stretching mode, as a function of the Valp:DMPC molar ratio, when Valp was incorporated into the lipid bilayer, in the gel (a) and liquid crystalline (b) state.

In the gel and liquid crystalline states, the contribution of $C = O_{bond}$ population is greater than that of $C{=}O_{free}$ for all Valp:DMPC molar ratios. The population of the $C{=}O_{bond}$ decreases with respect to the value of the pure lipid at the molar ratios 0.42: 1 and 0.84:1 while this trend is reversed for the molar ratio 1.69:1. This could indicate that Valp extracts the structured water from the population of the $C{=}O_{bond}$ which is reflected in the decrease in its percentage with respect to the pure lipid. Moreover, the interaction $C{=}O_{Valp}$ could take place for the Valp: DMPC molar ratio of 1.69:1.

The percentage of $C{=}O_{free}$ population increases slightly with respect to the value of the pure lipid and remains practically constant at all molar ratios tested, either in the gel or in the crystalline liquid state.

*3.1.3.3. $PO_2^-$ group*. In fully hydrated phosphatidylcholine in the liquid crystalline state, the characteristic phosphate group vibrational bands assigned to the $PO_2^-$ antisymmetric stretching mode ($\nu_{as}$ $PO_2^-$) is centered at 1229.5 $cm^{-1}$ and the $PO_2^-$ symmetric stretching mode ($\nu_s$ $PO_2^-$) at 1085.0 $cm^{-1}$. It is widely accepted that the frequency of the vibration ($\nu_{as}$ $PO_2^-$) is very sensitive to lipid hydration mainly because of direct H binding to the charged phosphate oxygen. Anhydrous lipid hydration displaces the band of the antisymmetric phosphate stretching to lower frequencies with increasing H-bonding (Lairion et al., 2006; Frías et al., 2007; Arias et al., 2018).

In MLVs of pure DMPC in the gel state (18 °C), the bands assigned to the anti-symmetric stretch mode of the $PO_2^-$ ($\nu_{as}$ $PO_2^-$) group are centered at 1213 $cm^{-1}$ and those of the symmetric stretch of the $PO_2^-$ ($\nu_s$ $PO_2^-$) at 1087 $cm^{-1}$. In crystalline liquid state, the bands are centered at 1212 $cm^{-1}$ for $\nu_{as}$ $PO_2^-$ and 1087 $cm^{-1}$ for $\nu_s$ $PO_2^-$.

In Tables S5 and S6 we present the assignments of the bands corresponding to the symmetric and antisymmetric stretches of the phosphate group, in MLVs of Valp:DMPC complexes and the changes in the wavenumbers with respect to pure DMPC, both for the gel state (18 °C) and for the liquid crystalline state (31 °C).

From the analysis of Tables S5 and S6, it is observed that the wavenumbers corresponding to the antisymmetric stretching mode of the phosphate group are displaced towards higher values. The extent of the shift towards higher values of the wavenumber is an indicator of the degree of dehydration of the phosphate group. On the other hand, for the symmetric stretch mode of the phosphate group, no significant interactions are observed in the different Valp: DMPC complexes. In addition, this effect is more noticeable in vesicles of DMPC resuspended in 7 mM Valp solution (Valp:DMPC molar ratio 0.094:1, Table S6) indicating a strong dehydration of the phosphate group without formation of H bond. In this system, the magnitude of the degree of dehydration ($\approx 18$ $cm^{-1}$) is similar for both states, gel and crystalline liquid.

This suggests that the effect of dehydration is due to the Valp in solution and does not synergize with the change in temperature, when passing from the gel to the liquid crystalline state. This effect is lower in the Valp:DMPC complexes incorporated directly in the membrane (Table S5), the magnitude of the dehydration is reflected in the changes in the wavenumbers that were approximately 4 $cm^{-1}$ for the gel and 4 to 7 $cm^{-1}$ for the crystalline liquid state.

In the case of liposomes resuspended in Valp solution, the dehydration could be due to an osmotic effect caused by the Valp action of sequestering structured water molecules of the phosphate groups. On the other hand, in systems where the Valp was incorporated into the membrane before forming the liposomes, the dehydration could be explained by the steric effect of the Valp molecules located in the interphasial region of the lipid bilayer.

Figs. 8 and 9 show in bar graphs the displacements in the

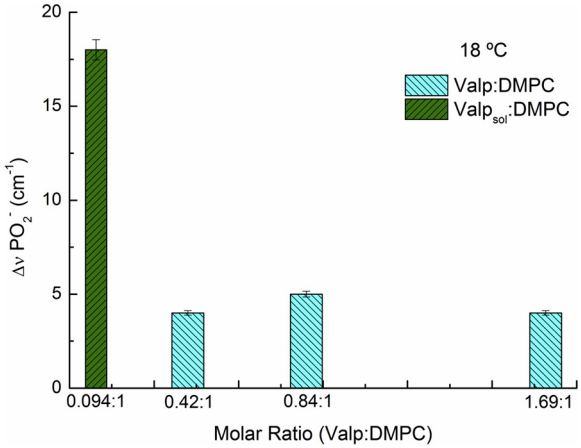


**Fig. 8.** Effect of Valp on the position of the vibrational bands of FTIR for the $PO_2^-$ group in DMPC, in gel state (18 °C).

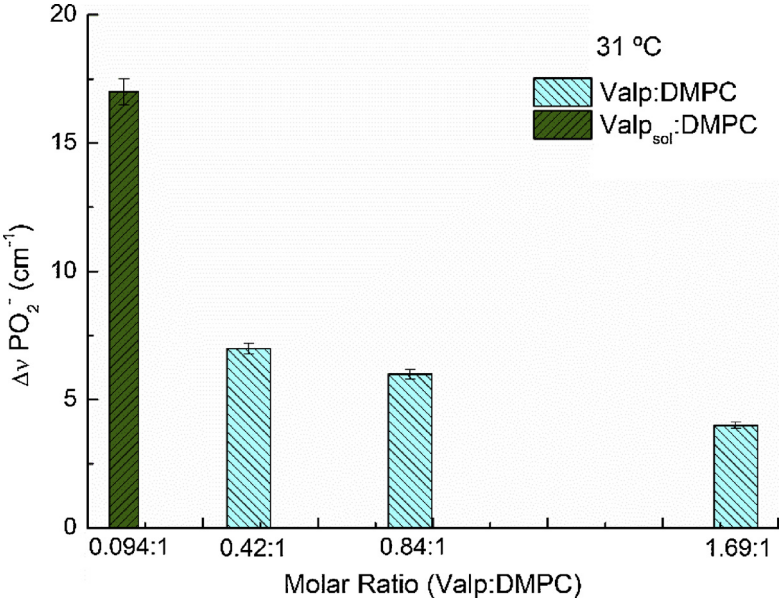


**Fig. 9.** Effect of Valp on the position of the vibrational bands of FTIR for the $PO_2^-$ groups in DMPC, in crystalline liquid state (31 °C).

wavenumbers of the asymmetric stretch of the $PO_2^-$ group due to the effect produced by Valp in the MLVs of Valp:DMPC complexes, in both states.

*3.1.3.4. Raman measurements*. Fig. 10 shows the Raman spectra of pure DMPC and the Valp:DMPC complexes, obtained at room temperature, at which the lipid is in the crystalline liquid state. The corresponding signals are assigned to the vibrations of the groups of the regions included between 2800 $cm^{-1}$ to 3000 $cm^{-1}$ and between 1000 $cm^{-1}$ to 1800 $cm^{-1}$.

The Raman assignments for the vibrational bands of the stretches $\nu_sCH_3$, $\nu_{as}CH_2$, $\nu_sCH_2$ and the change in the corresponding wavenumber are reported in Table S7. Displacements are observed for the higher frequencies (≈7 to 9 $cm^{-1}$) in the symmetric stretches of the terminal $CH_3$ groups and smaller displacements in the symmetric stretches of the $CH_2$ groups of the hydrocarbon chains of the lipids.

The region between 1000 $cm^{-1}$ and 1200 $cm^{-1}$ corresponds to the vibrational stretching of the C—C bonds of the acyl phospholipids chains. In the case of DMPC, the peaks at 1122 $cm^{-1}$ and 1062 $cm^{-1}$ are assigned to the stretches of the *trans* conformations, while the peak at 1087 $cm^{-1}$ to the *gauche* conformation (Lhert et al., 2000). The

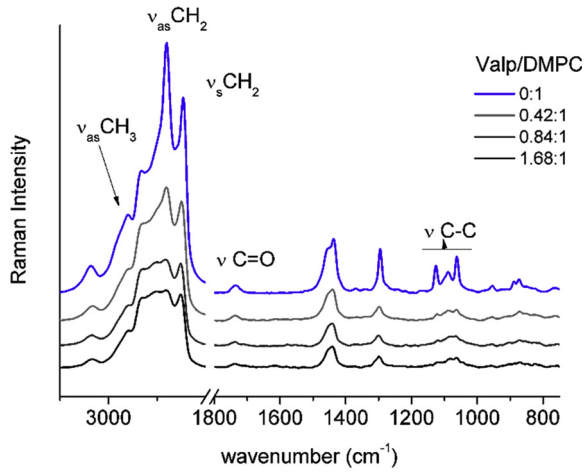


**Fig. 10.** Raman spectra of multilamellar vesicles of pure DMPC and complexes Valp:DMPC at room temperature.

intensity ratio $I_{1087\ (G)}$ / $I_{1062\ (T)}$ is a parameter that indicates the relative number of *gauche/trans* rotamers in the acyl phospholipids chains.

The intensity ratios of other bands of interest are: $I\nu_sCH_3/I\nu_sCH_2$ ($I_{2926}/I_{2850}$) and $I\nu_{as}CH_2/I\nu_sCH_2$ ($I_{2882}/I_{2850}$), which indicate the interaction between the hydrocarbon chains and give information on the coupling of the chains, respectively (Orendorff et al., 2002).

Analyzing the ratio of intensities $I_{1087\ (G)}/I_{1062\ (T)}$, it is observed that there is practically no change in the relative amount of *gauche* rotamers (G) with respect to *trans* (T). An increase in the ratio of intensities: $I\nu_sCH_3$ / $I\nu_sCH_2$greater than 0.3 in the Valp: DMPC complexes, indicates the increase in the degrees of freedom of rotation and vibration of the terminal methyl groups. In turn, the decoupling of hydrocarbon chains takes place. A decrease of ≈ 0.1 in the ratio of intensities: $I\nu_{as}CH_2/I\nu_sCH_2$ ($I_{2882}/I_{2850}$), would indicate that there is a slight decrease in the order or coupling of chains (Figure S6).

### 3.2. Electrochemical characterization of the Au/SLB systems

Results obtained by using electrochemical measurements describe the changes in the electrical properties of supported bilayers that result from variations in the conditions under which the bilayers interact with valproic acid. We can discuss the findings mainly, in terms of induced membrane defects. These defects are facilitated paths for species of the electrolyte to cross the barrier set up by the bilayer and to produce a faradaic current. In other words, the defects are associated with an increase in the membrane permeability. Within this framework, the important role of the electrostatics of the solid substrate/lipid bilayer system in the presence of valproic acid is readily identified. Thus, an increase in permeability is the result of alterations of the structure of the lipid bilayer with a consequent degradation of its insulating properties. An increase in bilayer permeability correlates with larger voltammetric peak currents. Moreover, impedance-derived parameters such as resistance and capacitance of the membrane are also very useful to assess changes in permeability as discussed below. For a detailed description of how the analysis of the experimental results is performed, the reader is referred to the work by Wiegand et al (Wiegand et al., 2002).

Fig. 11 shows voltammograms for Au substrates modified with supported lipid bilayers of DMPC in buffer Tris 10 mM containing KCl 0.1 M at pH = 7.4 (black line), and in buffer Tris 10 mM containing KCl

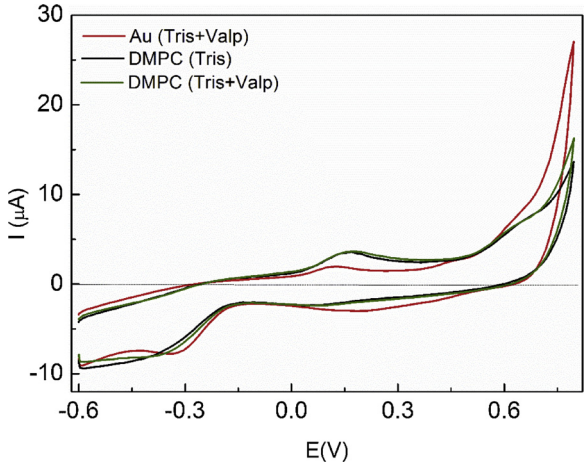


**Fig. 11.** Cyclic voltammograms for gold electrodes modified with SLBs of DMPC in solutions of: buffer Tris 10 mM containing KCl 0.1 M at pH = 7.4 (black line) and buffer Tris 10 mM containing KCl 0.1 M and valproic acid (Valp) 7 mM (green line). Cyclic voltammogram for a gold electrode in buffer Tris 10 mM with KCl 0.1 M and Valp 7 mM at pH = 7.4 (red line). All voltammograms were recorded at a scan rate v = 50 $mVs^{-1}$, at 25 °C in the potential window with $E_{s,c}$ = – 0.6 V and $E_{s,a}$ = 0.8 V scan limit values.

0.1 M and valproic acid (Valp) 7 mM (green line). The red line plot corresponds to the voltammetric response of a Au surface in a solution of buffer Tris 10 mM with KCl 0.1 M and Valp 7 mM at pH = 7.4. The scan rate was v = 50 $mVs^{-1}$ and the cathodic and anodic switching potentials were $E_{s,c}$ = –0.600 V and $E_{s,a}$ = 0.800 V, respectively. A negligible change of the voltammetric profile for the electrode modified with the SLB can be observed resulting from the presence of Valp in the electrolyte. Moreover, no redox reaction related to Valp can be found in the studied potential window.

The voltammetric response of Au-DMPC can be seen in Fig. 12 together with the voltammograms for Au electrodes modified with SLBs of DMPC doped with Valp according to the following three molar ratios: $Valp_1$:DMPC (0.42:1), $Valp_2$:DMPC (0.84:1) y $Valp_3$:DMPC (1.68:1). Voltammograms in Fig. 12 were recorded in solution of Tris 10 mM and KCl 0.1 M, pH = 7.4 at 25 °C. The presence of Valp in the membrane determines slightly enhanced redox contributions according to the Valp

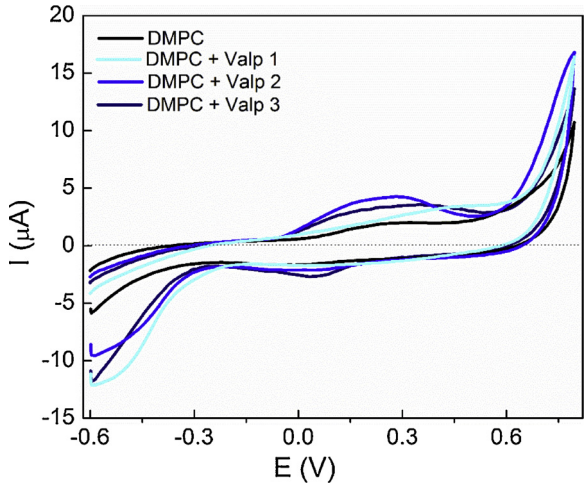


**Fig. 12.** Voltammograms for Au-DMPC (black) and Au substrates modified with SLBs of DMPC doped with Valp according to the following three molar ratios: $Valp_1$:DMPC (0.42:1) (cyan), $Valp_2$:DMPC (0.84:1) (blue) and $Valp_3$:DMPC (1.68:1) (dark blue). Voltammograms were recorded in solution of Tris 10 mM and KCl 0.1 M, at 25 °C with v = 50 $mVs^{-1}$, in the scan range from $E_{s,c}$ = – 0.6 V to $E_{s,a}$ = 0.8 V.

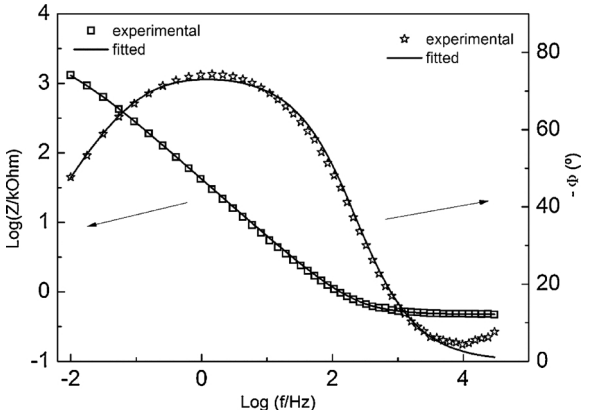


**Fig. 13.** Bode plots of impedance data (experimental and fitted) for a Au + DMPC electrode in solution of buffer Tris 10 mM + KCl 0.1 M.

molar ratio. This suggests that an increase in the number of membrane defects occurs related to the interaction of Valp with the SLBs.

Impedance spectra are shown in Fig. 13 as Bode plots for the experimental data together with the results from the fitting procedure. Experimental spectra were recorded with an Au-DMPC electrode in solution of buffer Tris 10 mM + KCl 0.1 M. These data were fitted to the theoretical impedance of the equivalent circuit shown in Fig. 14.

The equivalent circuit shown in Fig. 14 (Diamanti et al., 2016) was selected to fit the experimental impedance spectra. It contains a series connection of the electrolyte resistance $R_1$ and two impedance elements, each one containing a parallel connection of a capacitance and a resistance. The lipid membrane parameters are the capacitance C and the resistance $R_3$. A constant phase element (CPE) Q (corresponding to a capacitance as a distributed property) in parallel connection with a resistance $R_2$ represent the impedance of the hydrophilic spacer on top of which the bilayer membrane is supported, as described above. In this study the capacitance C and resistance $R_3$ of the bilayer membrane are the most important parameters to be derive by using EIS.

Fig. 15 shows impedance spectra for Au-DMPC electrodes in solution of buffer Tris 10 mM + KCl 0.1 M + Valp 7 mM, at pH = 7.4 and 25 °C. Theoretical curves were obtained through data fitting and the best-fit parameters were assembled in Table 1 together with parameters corresponding to Au-DMPC electrodes in solution of buffer Tris 10 mM + KCl 0.1 M in the absence of Valp.

Equation 1shows the relationship between the membrane capacitance C and their related dielectric properties (Flynn et al., 2018)

$$C = \frac{\varepsilon\varepsilon o}{L} \quad (1)$$

where the dielectric constant of the bilayer ε is a function of the frequency and membrane composition and structure, εo is the dielectric permittivity of vacuum (9.8542 × $10^{-12}$ F $m^{-1}$), and L is the thickness of the membrane. From this equation it is apparent that the membrane

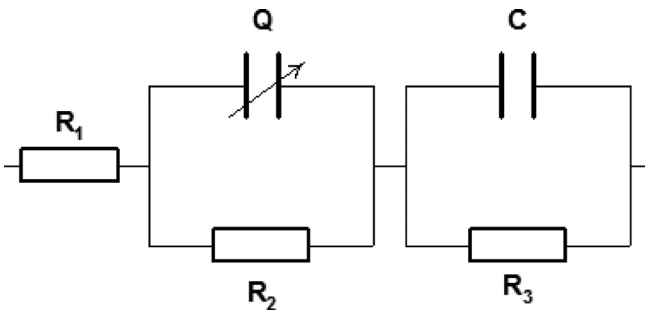


**Fig. 14.** Equivalent circuit used in the fitting procedure of experimental impedance spectra recorded for Au substrates modified with a DMPC bilayer.

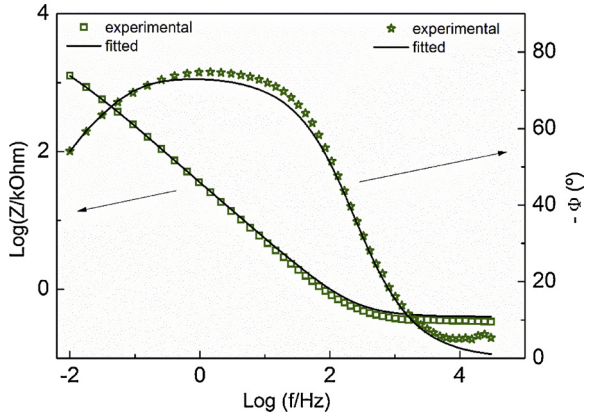


**Fig. 15.** Experimental and theoretical Bode plots for Au-DMPC electrodes in solution of buffer Tris 10 mM + KCl 0.1 M + Valp 7 mM, at pH = 7.4 and 25 °C.

**Table 1**
Best fit parameters derived from the fitting procedure for experimental spectra in Figs. 13 and 15.

| | C/F $cm^{-2}$ | $R_3/\Omega\ cm^2$ | $A_p/A_e$ |
|---|---|---|---|
| Au-DMPC | $2.11\ 10^{-5}$ | $1.80\ 10^{6}$ | $4.63\ 10^{-12}$ |
| Au-DMPC in (Tris + $Valp_{sol}$) | $6.66\ 10^{-5}$ | $7.04\ 10^{4}$ | $1.18\ 10^{-10}$ |

capacitance will be affected by changes in both L and ε.

The resistance of the membrane $R_3$ is determined by the electrolyte-filled pores spanning the bilayer thickness. Thus, we can calculate the relative pore area fraction as usual:

$$R_3/A_e = r_o\ L/A_p \quad (2)$$

where, the thickness of the membrane L = 5 nm, $A_p$ is the pore area, $A_e$ is the geometric area of the Au electrode and $r_o$ is the resistivity of the electrolyte solution (16.67 Ω cm) (Cassier et al., 1999). Accordingly, area ratios $A_p/A_e$ included in Table 1 were calculated according to Eq. (2).

Fig. 16 displays impedance data for Au substrates modified with DMPC lipid bilayers which were doped with Valp according to a molar ratio $Valp_2$:DMPC (0.84:1). The experimental spectrum was recorded in solution of buffer Tris 10 mM + KCl 0.1 M. Theoretical plots result from data fit to the impedance of the equivalent circuit in Fig. 14.

The best-fit values for the membrane parameters are shown in

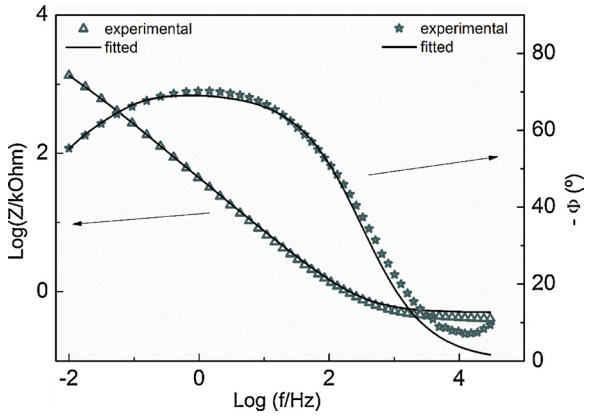


**Fig. 16.** Experimental and fitted Bode plots for Au substrates modified with DMPC lipid bilayers doped with Valp according to the molar ratio $Valp_2$:DMPC (0.84:1). Experimental data were recorded in solution of buffer Tris 10 mM + KCl 0.1 M. Theoretical plots result from data fitting with the equivalent circuit in Fig. 14.

**Table 2**
Best-fit parameters for impedance data of Au substrates modified with DMPC lipid membranes doped with Valp according to the molar ratios $Valp_1$:DMPC (0.42:1), $Valp_2$:DMPC (0.84:1) and $Valp_3$:DMPC (1.68:1).

| | C/Fcm$^{-2}$ | $R_3/cm^2$ | $A_p/A_e$ |
|---|---|---|---|
| $Valp_1$ | $2.97\ 10^{-5}$ | $8.17\ 10^{4}$ | $1.02\ 10^{-10}$ |
| $Valp_2$ | $7.81\ 10^{-5}$ | $4.93\ 10^{4}$ | $1.69\ 10^{-10}$ |
| $Valp_3$ | $6.48\ 10^{-5}$ | $4.86\ 10^{4}$ | $1.71\ 10^{-10}$ |

Table 2. Experimental impedance spectra were obtained with Au substrates modified with DMPC lipid bilayers doped with Valp according to three Valp:DMPC molar ratios. Also included in the table is the relative pore area fraction $A_p/A_e$. An increase in $A_p/A_e$ can be observed after doping the membrane with Valp (compare with the value for an undoped membrane in Table 1). Also an increase in $A_p/A_e$ results for increasing Valp:DMPC molar ratios.

The interaction of Valp with the studied lipid membranes is characterized by a decrease in the membrane resistance values. This effect is more marked when the biomolecule is incorporated into the lipid structure as compared with the situation when Valp is present in the electrolyte solution.

As for the membrane capacitance, the interaction of Valp with the lipid membrane results in an increase in its value, for both experimental conditions (incorporated into the lipid and present in the solution). A larger membrane capacitance can be understood in terms of a lipid membrane with a larger number of defects and a larger dielectric constant (as in the case of the biomolecule incorporation into the hydrophobic region of the membrane).

## 4. Conclusions

No change was observed in the $T_m$ of DMPC when the MLVs are resuspended in the valproic acid solution, even for long exposure times after the vesicles were formed. In addition, no modification was detected in the sigmoidal shape of the plot showing the symmetric stretching of the $CH_2$ group according to the temperature. The Valp in solution seems to maintain the same conformational characteristics in the lipid bilayer core with respect to the DMPC pure stabilized in water. These results suggest that the Valp in solution could stabilize the core DMPC liposomes under the conditions tested.

On the other hand, complex effects related to Valp incorporation into the lipid vesicles were observed. As the Valp:DMPC ratio increases Tm decreases and the phase transition becomes less noticeable. For the Valp:DMPC complex species a slight decrease in the number of *gauche* isomers was observed compared with the number of *trans* isomers what corresponds to an increase in the packing density of the acylic chains. For the Valp:DMPC complex species with a molar ratio larger than 0.6:1 a decrease in the frequency of molecular interactions can be observed. This effect results from an increase in the rotational and vibrational degrees of freedom of the terminal methyl groups as the chains are decoupled. It can be inferred that the incorporation of Valp forming the Valp: DMPC complexes alters the fluidity of the lipid membrane (order of the hydrocarbon chains).

In the interphasial region, a displacement of structured water molecules was observed for the population of the bonded carbonyl group, with subsequent formation of hydrogen bonds in the gel state. The percentage of the population of the $C = O_{bond}$ groups in the interphasial region decreases at low molar ratios, inverting the trend for the highest molar ratio of the Valp: DMPC complex. This could result in the interaction C═O—Valp, in both gel and crystalline liquid states. Valp would have greater access to the C═O groups, replacing the water of hydration in the interphasial region of the lipid with subsequent formation of hydrogen bonds. In the hydrophilic region of the lipid, the changes observed in the polar head group can be understood as

replacement of water molecules in the hydration layer, specifically in the $PO_2^-$ group, without further formation of hydrogen bonds with Valp molecules.

The interaction of Valp with the lipid membrane results in lower values for the membrane resistance, especially in the case when Val was incorporated into the membrane.

An increase in the capacitance values was observed related to the interaction of Valp with the lipid membrane under both experimental conditions, namely, when Valp is incorporated into the lipid and when it is dissolved in the solution. Larger capacitance values are usually associated with a larger number of defects and a larger dielectric constant, as in the case of the biomolecule incorporation into the membrane hydrophobic region.

The changes in the capacity of the lipid membrane and in its dielectric constant, in the presence of Valp molecules, could be related to the dehydration effect of the polar head groups of the phospholipids in the Valp: DMPC complexes.

## Conflict of interest

The authors certify that there is no conflict of interest with any financial/research/academic organization, concerning the content discussed in the manuscript.

## Funding

The authors gratefully acknowledge the Consejo de Investigaciones de la Universidad Nacional de Tucumán (CIUNT). This work was supported by the Agencia Nacional de Promoción Científica y Tecnológica with grants PICT Nº 2008-1902 and PICT Nº 2014-1785.

## Acknowledgments

C.A. Gervasi gratefully acknowledges the Comisión de Investigaciones Científicas y Técnicas Buenos Aires (CICBA) for his position as a member of the Carrera del Investigador Científico. A. Ben Altabef is a member of the Research Career of CONICET (Argentina).

## Appendix A. Supplementary data

Supplementary data associated with this article can be found, in the online version, at https://doi.org/10.1016/j.chemphyslip.2018.12.010.

## References

Alvarez, P.E., Gervasi, C.A., Vallejo, A.E., 2007. Impedance analysis of ion transport through supported lipid membranes doped with ionophores: a new kinetic approach. J. Biol. Phys. 33, 421–431.
Arias, J.M., Tuttolomondo, M.E., Díaz, Sonia B., Ben Altabef, A., 2015. FTIR and Raman analysis ofL-cysteine ethyl ester HCl interaction with dipalmitoylphosphatidylcholine in anhydrous and hydrated states. J. Raman Spectrosc. 46 (4), 369–376.
Arias, J.M., Tuttolomondo, M.E., Díaz, S.B., Ben Altabef, A., 2018. Reorganization of hydration water of DPPC multilamellar vesicles induced by L-Cysteine interaction. J. Phys. Chem. B 122, 5193–5204.
Bangham, A.D., Hill, M.W., Miller, N.G.A., 1974. Preparation and use of liposomes as models of biological membranes. Methods in membrane biology. In: Korn, E.D. (Ed.), Methods in Membrane Biology. Plenum Press, New York, pp. 1–61.
Bergera, N., Sachse, A., Bender, J., Schubert, R., Brandl, M., 2001. Filter extrusion of liposomes using different devices: comparison of liposome size, encapsulation efficiency, and process characteristics. Int. J. Pharm. 223, 55–68.
Bilge, D., Kazanci, N., Severcan, F., 2013. Acyl chain length and charge effect on Tamoxifen–lipid model membrane interactions. J. Mol. Struct. 1040, 75–82.
Cameron, D.G., Casal, H.L., Mantsch, H.H., 1980. Characterization of the pretransition in 1,2-dipalmitoyl-sn-glycero-3-phosphocholine by Fourier transform infrared spectroscopy. Biochemistry 19, 3665–3672.
Casal, H.L., Mantsch, H.H., 1984. Polymorphic phase behaviour of phospholipid membranes studied by infrared spectroscopy. Biochim. Biophys. Acta 779, 381–401.
Cassier, T., Sinner, A., Offenhäuser, A., Möhwald, H., 1999. Homogeneity, electrical resistivity and lateral diffusion of lipid bilayers coupled to polyelectrolyte multilayers. Colloids Surf. B Biointerfaces 15, 215–225.
Chan, Y.-H.M., Boxer, S.G., 2007. Model membrane systems and their applications. Curr. Opin. Chem. Biol. 11, 581–587.
Corrales Chahar, F., Díaz, S.B., Ben Altabef, A., Gervasi, C.A., Alvarez, P.E., 2018. Characterization of interactions of eggPC lipid structures with diferent biomolecules. Chem. Phys. Lipids 210, 60–69.
Cortijo, M., Chapman, D., 1981. A comparison of the interactions of cholesterol and gramicidin a with lipid bilayers using an infrared data station. FEBS Lett. 131, 245–248.
Diamanti, E., Azzaroni, O., Gregurec, D., Moya, S.E., Rodríguez-Presa, M.J., Gervasi, C.A., 2016. High resistivity lipid bilayers assembled on polyelectrolyte multilayer cushions: an impedance study. Langmuir 32, 6263–6271.
Diamanti, E., Gutiérrez-Pineda, E., Politakos, N., Andreozzi, P., Rodriguez-Presa, M.J., Knoll, W., Azzaroni, O., Gervasi, C.A., Moya, S., 2017. Gramicidin ion channels in a lipid bilayer supported on polyelectrolyte multilayer films: an electrochemical impedance study. Soft Matter 13, 8922–8929.
Dıaz, S.B., Biondi de Lopez, A.C., Disalvo, E.A., 2003. Dehydration of carbonyls and phosphates of phosphatidylcholines determines the lytic action of lysoderivatives. Chem. Phys. Lipids 122, 153–157.
Disalvo, E.A., Lairion, F., Díaz, S.B., Arroyo, J., 2002. Physical chemistry of lipid interfaces: state of hydration, topological and electrical properties. In: Condat, C.A., Baruzzi, A. (Eds.), Recent Research Developments in Biophysical Chemistry, Research Signpost, India.
Disalvo, E.A., Lairion, F., Martini, F., Tymczyszyn, E., Frías, M., Almaleck, H., Gordillo, G.J., 2008. Structural and functional properties of hydration and confined water in membrane interfaces. Biochim. Biophys. Acta 1778, 2655–2670.
Du, L., Liu, X., Huang, W., Wang, E., 2006. A study on the interaction between ibuprofen and bilayer lipid membrane. Electrochim. Acta 51, 5754–5760.
El Kirat, K., Morandat, S., Dufrêne, Y.F., 2010. Nanoscale analysis of supported lipid bilayers using atomic force microscopy. Biochimica et Biophysica Acta 1798, 750–765.
Ergun, S., Demir, P., Uzbay, T., Severcan, F., 2014. Agomelatine strongly interacts with zwitterionic DPPC and charged DPPG membranes. Biochimica et Biophysica Acta 1838, 2798–2806.
Flynn, K.R., Leigh Ackland, M., Torriero, A.A.J., 2018. Electrochemical impedance spectroscopy study of the interaction of supported lipid bilayers with free docosahexaenoic acid. Med. Anal. Chem. Int. J. 2 (3), 000122.
Frías, M.A., Nicastro, A., Casado, N.M.C., Gennaro, A.M., Díaz, S.B., Disalvo, E.A., 2007. Arbutin blocks defects in the ripple phase of DMPC bilayers by changing carbonyl organization. Chem. Phys. Lipids 147, 22–29.
Garcia-Manyes, S., Oncins, G., Sanz, F., 2005. Effect of temperature on the nanomechanics of lipid bilayers studied by force spectroscopy. Biophys. J. 89, 4261–4274.
Heimburg, T., 2007. Tutorials in Biophysics: Thermal Biophysics of Membranes. WILEY-VCH Verlag GmbH & Co., KGaA, Weinheim, pp. 1–378.
Johannessen, C.U., Johannessen, S.I., 2003. Valproate: past, present, and future. CNS Drug Rev. 9 (2), 199–216.
Juhaniewicz, J., Sek, S., 2015. Atomic force microscopy and electrochemical studies of melittin action on lipid bilayers supported on gold electrodes. Electrochim. Acta 162, 53–61.
Keane, P.E., Simiand, J.E., Mendes, Santucci, V., Morre, M., 1983. The effects of analogues of valproic acid on seizures induced by pentylenetetrazol and GABA content in brain of mice. Neuropharmacology 22, 879.
Kessel, A., Musafia, B., Ben-Tal, N., 2001. Continuum solvent model studies of the interactions of an anticonvulsant drug with a lipid bilayer. Biophys. J. 80, 2536–2545.
Lairion, F., Martini, F., Díaz, S., Brandán, S., Ben Altabef, A., Disalvo, E.A., 2006. Chapter 34: modulation of the hydration of lipid membrane phosphates by choline, glycerol, and ethanolamine groups. In: In: del Pilar Buera, M., Welti-Chanes, J., Lillford, P.J., Corti, H.R. (Eds.), Water Properties of Food, Pharmaceutical, and Biological Materials 9. CRC Press, Boca Raton, Florida, USA, pp. 503–511 Collection: Food Preservation Technology.
Lhert, F., Capelle, F., Blaudez, D., Heywang, C., Turlet, J.-M., 2000. Raman spectroscopy of phospholipids black films. J. Phys. Chem. 104, 11704–11707.
Lin, M.W., Huang, Y.B., Chen, C.L., Wu, P.C., Chou, Ch.Y., Wu, P.C., Hung, S.Y., 2016. A formulation study of 5-Aminolevulinic encapsulated in DPPC liposomes in melanoma treatment. Int. J. Med. Sci. 13 (7), 483–489.
Loscher, W., 1999. Valproate: a reappraisal of its pharmacodynamics properties and mechanisms ofaction. Prog. Neurobiol. 58, 31–59.
Lyon, R.C., Goldstein, D.B., 1980. The comparative effects of sodium valproate, sodium octanoate, and sodium valerate on spin-labeled synaptosomal plasma membrane from mouse brain. Fed. Proc. 39, 1100.
MacCallum, J.L., Tieleman, D.P., 2008. Interactions between small molecules and lipid bilayers. Chapter 8 In: Feller, Scott E. (Ed.), Current Topics in Membranes, 60. Elsevier, New York, pp. 227–60256 and references therein.
Mannock, D.A., Lewis, R.N.A.H., McElhaney, R.N., 2006. Comparative calorimetric and spectroscopic studies of the effects of Lanosterol and cholesterol on the thermotropic phase behavior and organization of dipalmitoylphosphatidylcholine bilayer membranes. Biophys. J. 91, 3327–3340.
Martin, D.K., 2007. The significance of biomimetic membrane nanobiotechonology to biomedical applications. In: Martin, D.K. (Ed.), Nanobiotechnology of Biomimetic Membranes. Springer, New York, pp. 1–21.
Olson, F., Hunt, C.A., Szoka, F.C., Vail, W.J., Papahadjopoulos, D., 1979. Preparation of liposomes of defined size distribution by extrusion through polycarbonate membranes. Biochimica et Biophysica Acta 557, 9–23.
Orendorff, C.J., Ducey, M.W., Pemberton, J.E., 2002. Quantitative correlation of raman spectral indicators in determining conformational order in alkyl chains. J. Phys. Chem. A 106, 6991–6998.
Plant, A.L., 1993. Self-assembled Phospholipid/Alkanethiol biomimetic bilayers on gold. Langmuir 9, 2764–2767.
Purrucker, O., Hillebrandt, H., Adlkofer, K., Tanaka, M., 2001. Deposition of highly

resistive lipid bilayer on silicon-silicon dioxide electrode and incorporation of gramicidin studied by ac impedance spectroscopy. Electrochim. Acta 47, 791–798.
Rameshkumar, S., Kumaravel, M., 2017. Changes in the electrical properties of agargel supported bilayer lipid membrane brought about by midazolam. Electrochim. Acta 251, 189–196.
Rosenberg, G., 2007. The mechanisms of action of valproate in neuropsychiatric disorders: can we see the forest for the trees? Review. Cell. Mol. Life Sci. 64, 2090–2103.
Steinem, C., Galla, H.-J., Jansho, A., 2000. Interaction of melittin with solid supported membranes. Phys. Chem. Chem. Phys. 2, 4580–4585.
Ulander, J., Haymet, A.D.J., 2003. Permeation Across Hydrated DPPC Lipid Bilayers: Simulation of the Titrable Amphiphilic Drug Valproic Acid. Biophys. J. 85, 3475–3484.
Vallejo, A.E., Gervasi, C.A., 2006. On the use of impedance spectroscopy for studying bilayer lipid membranes. In: In: Leimannova Liu, A. (Ed.), Advances in Planar Lipid Bilayers and Liposomes 3. Elsevier, Amsterdam, pp. 331–353.
Wiegand, G., Arribas-Layton, N., Hillebrandt, H., Sackmann, E., Wagner, P., 2002. Electrical properties of supported lipid bilayer membranes. J. Phys. Chem. B 106, 4245–4254.
Ziebert, F., Lacoste, D., 2011. A planar lipid bilayer in an electric Field: membrane instability, Flow Field, and electrical impedance. In: In: Leimannova Liu, A. (Ed.), Advances in Planar Lipid Bilayers and Liposomes 14. Elsevier, Amsterdam, pp. 63–95.